

Accepted Manuscript

Title: BiVO₄/g-C₃N₄ composite visible-light photocatalyst for effective elimination of aqueous organic pollutants

Author: Jie Zhao Jinghui Yan Huaijie Jia Shaowei Zhong
Xinyan Zhang Lei Xu



PII: S1381-1169(16)30360-0
DOI: <http://dx.doi.org/doi:10.1016/j.molcata.2016.08.025>
Reference: MOLCAA 10012

To appear in: *Journal of Molecular Catalysis A: Chemical*

Received date: 23-6-2016
Revised date: 22-8-2016
Accepted date: 24-8-2016

Please cite this article as: Jie Zhao, Jinghui Yan, Huaijie Jia, Shaowei Zhong, Xinyan Zhang, Lei Xu, BiVO₄/g-C₃N₄ composite visible-light photocatalyst for effective elimination of aqueous organic pollutants, *Journal of Molecular Catalysis A: Chemical* <http://dx.doi.org/10.1016/j.molcata.2016.08.025>

This is a PDF file of an unedited manuscript that has been accepted for publication. As a service to our customers we are providing this early version of the manuscript. The manuscript will undergo copyediting, typesetting, and review of the resulting proof before it is published in its final form. Please note that during the production process errors may be discovered which could affect the content, and all legal disclaimers that apply to the journal pertain.

<AT>BiVO₄/g-C₃N₄ composite visible-light photocatalyst for effective elimination of aqueous organic pollutants

<AU>Jie Zhao, Jinghui Yan, Huaijie Jia, Shaowei Zhong, Xinyan Zhang*
##Email##zhangxinyan@hotmail.com##/Email##, Lei Xu**
##Email##xul646@163.com##/Email##

<AU>

<AFF>School of Chemistry and Environmental Engineering, Changchun University of Science and Technology, Changchun 130022, PR China

<PA>*Corresponding authors: Tel/ Fax: +86-431-8558-312 <PA>**Corresponding authors: Tel/ Fax: +86-431-8558-3152.

<ABS-Head><ABS-HEAD>Graphical abstract

<ABS-P>

<ABS-P><xps:span class="xps_Image">fx1</xps:span>

<ABS-HEAD>Highlights ► BiVO₄/g-C₃N₄ composite photocatalysts were synthesized by sonification method. ► 10 wt.% BiVO₄/g-C₃N₄ catalyst exhibited excellent degradation efficiency towards RhB or PNP. ► Enhanced activity of BiVO₄ is ascribed to better optical utilization, adsorption ability and lower electron-hole pairs recombination rate. ► •OH radical is also active species in BiVO₄/g-C₃N₄-based visible-light system. ► 10 wt.% BiVO₄/g-C₃N₄ showing great potential for aqueous organic contaminants elimination in future applications.

<ABS-HEAD>Abstract

<ABS-P>BiVO₄/g-C₃N₄ composite photocatalysts were successfully synthesized by sonification and the chemical structures of BiVO₄/g-C₃N₄ heterostructures are characterized systematically. The photocatalytic activity of BiVO₄/g-C₃N₄ for rhodamine B (RhB) and *p*-nitrophenol (PNP) degradation is evaluated under visible light irradiation. It has been found that the novel BiVO₄/g-C₃N₄ composites exhibit excellent catalytic activities towards RhB and PNP degradation, and these BiVO₄/g-C₃N₄ composites are much more active compared with that of pure g-C₃N₄. Activity enhancement after BiVO₄ introducing is mainly attributed to the better optical

absorption ability over the well contacted structure in heterojunctions, good adsorption ability of organic contaminants and lower recombination rate of electron-hole pairs. In addition, in BiVO₄/g-C₃N₄-based visible-light system •OH radical, not active in pure g-C₃N₄ system, is also found to be active species for pollutants degradation, which maybe another evidence for the enhanced photocatalytic activity by BiVO₄ introduction. Furthermore, the most active 10 wt.% BiVO₄/g-C₃N₄ photocatalyst exhibits enough catalytic stability in recycle test, showing great potential as cost-effective heterogeneous visible-light photocatalyst for aqueous organic contaminants elimination in future applications.

<KWD>Keywords: G-C₃N₄; Photocatalysis; Heterostructure; BiVO₄; Sonification

<H1>1. Introduction

In recent times, the increasing environmental issues have become great threaten to the modern society. Photocatalytic technology based on semiconductor photocatalysis has been regarded as a promising alternative for environmental remediation, since it has the property of energy saving, avoidance of re-contamination and excellent photocatalytic property for organic pollutants degradation [1]. Of all photocatalysis reported, TiO₂ has probably attracted most attention because of its no toxicity, high durability and good photocatalytic performance. Nevertheless, the wide band gap of TiO₂ makes it only responsive to ultraviolet light, occupying below 4% of the solar spectrum. This drawback of TiO₂ greatly restricts its practical applications in environmental and energy area [2]. Consequently, lots of research have been carried

out to improve the solar light utilization level of photocatalysts, for instance to develop materials with visible light sensitivity and thus good photocatalysts activities for pollutants degradation under visible light irradiation [3]. In this aspect, g-C₃N₄ (graphite-like carbon nitride) emerges and has drawn increasing concern because it has high visible light absorption ability, good stability, and excellent visible-light photocatalytic activity on organic dyes removal [3-5]. Furthermore, the chemical component of g-C₃N₄ is inexpensive carbon and nitrogen and its preparation route is easy to implement [5]. All these features facilitates its practical applications in organic pollutants elimination. However, g-C₃N₄ still suffers from high recombination rate of photo-generated electron-hole pairs, which is an inherent and unavoidable defect of semiconductor based photocatalysis and this drawback greatly restricted the improvement in photocatalytic performance of g-C₃N₄ [6]. Consequently, great efforts have been made to enhance its charge separation efficiency and hence to increase its visible light photocatalytic activity. Several methods have been developed, including preparation of g-C₃N₄ with different morphology [7], doption of impurities components [8-9] and formation of composite structures [10-12]. Compared with other methods, forming composite heterojunction could utilize the structure merits of g-C₃N₄, i.e. large specific surface area and open texture with two-dimensional planar conjugation, and being a good supporter for other composite, thus efficient in improving visible light response. Several kinds of semiconductors have been reported to add to g-C₃N₄ and form a heterojunction system, such as ZnWO₄, Bi₂WO₆ and CdS, etc [10-12]. It is reported that there is synergistic effects between the g-C₃N₄ and

other materials with suitable band position and the recombination rate of photogenerated electron-hole pairs could be effectively suppressed in the composite heterojunction [10-12].

On the other hand, recently, monoclinic BiVO_4 , as a novel nontoxic and chemically stable semiconductor, has attracted increasing interests for its excellent photocatalytic performance for O_2 evolution under visible light irradiation [13]. BiVO_4 is found highly response to visible light because of its narrow band-gap of 2.42 eV[14], and could utilize visible light directly without modification. All these properties suggest that BiVO_4 would be a probable material with great promise for fabricating composite with other materials [4], although the photocatalytic efficiency of pure BiVO_4 in organic pollutants degradation is usually not satisfied enough due to its poor adsorption ability. Meanwhile, the energy levels of g- C_3N_4 and BiVO_4 are well-matched overlapping band-structures (both of the valence and conduction band levels of BiVO_4 is lower than that of g- C_3N_4) which make it highly possible to form BiVO_4 doped g- C_3N_4 heterojunction with excellent transfer and separation ability of electron-hole pairs in the heterojunction structure[15]. Furthermore, g- C_3N_4 has two-dimensional open structure and very large specific surface area, which would provide the BiVO_4 anchored g- C_3N_4 heterojunction with great dispersity and excellent adsorption ability, thus improved photocatalytic performance [4]. Indeed, most recently, a C_3N_4 - BiVO_4 heterojunction have been successfully prepared by mixing and heating method of C_3N_4 and BiVO_4 or hydrothermal route [16-17]. Nevertheless, the chemical status of contact interface of the obtained heterojunction is greatly relied

on the heating process involved, thus influence their photocatalytic performance. Motivated by this, we further research the preparation of BiVO₄ loaded C₃N₄ heterojunction by sonification method, which is superior in simple operation, green chemical process and especially good dispersion of component[18]. Furthermore, till now, there is not report on ultrasound assisted preparation of C₃N₄-BiVO₄ heterojunction yet as far as we know. The current study indicates that the novel C₃N₄-BiVO₄ composite photocatalyst could be successfully prepared by facile sonification method and exhibited excellent photocatalytic performance under visible light irradiation, showing great potential as cost-effective heterogeneous visible-light photocatalyst for aqueous organic contaminants elimination in future applications. Furthermore, the possible photocatalytic reaction mechanism on the C₃N₄-BiVO₄ heterojunction surface has been proposed based on systematical characterization results..

<H1>2. Experimental

<H2>2.1. Photocatalysts preparations

The pure g-C₃N₄ was prepared according the literature reported following the typical procedure [5]: urea was heated to 250 °C and kept for 1 h, to 350 °C and kept for 2 h and finally to 550 °C and kept for 2 h in a semi-closed alumina crucible with a cover. The product was thoroughly washed and dried at 80 °C overnight.

Pure Monoclinic BiVO₄ was prepared by hydrothermal method: Bi(NO₃)₃·5H₂O (1.21275 g) was added into 5 mL HNO₃ (4 mol/L) and vigorously stirred for 30 min, which was named solution A. NH₄VO₃ (0.2925 g) was put into concentrated 2 mol/L

NaOH(5 mL) solution(named as solution B) and stirred for 30 min. Subsequently, Solution B was added into solution A and stirred for another 1 h. After adjusting the acidity to pH 6, the mixture was transferred into a Teflon-lined stainless steel autoclave and heated to 150 °C and kept for 12 h, and then cooled down naturally. The yellow solid was thoroughly washed and dried at 80 °C overnight.

The BiVO₄/g-C₃N₄ composite with BiVO₄ loading varied from 10-30% was prepared by the typical procedure as follows: certain amounts of BiVO₄ and g-C₃N₄ were mixed in appropriate amount of distilled water, which was stirred for 10 min. Then the mixture was subjected to ultrasound irradiation for 1 h at 30±0 °C using a water and ice mixture. The composites were dried thoroughly in 80 °C overnight. Finally, the composites were collected and named as x wt.% BiVO₄/ g-C₃N₄, where x represents the BiVO₄ loading.

2.2. Material Characterization

The X-ray diffraction patterns were measured on a Rigaku powder diffractometer (D/MAX-RB, Cu K α , $\lambda=1.5418 \text{ \AA}$). FTIR spectra were obtained on the spectrometer (SHIMADZU FTIR-8400S). X-ray photoelectron spectroscopies were measured on a VG-ADES 400 IR spectrometer. The scanning electron microscope (SEM) images were determined by a JSM-6480 SEM spectrometer. The transmission electron microscope (TEM) images were determined by a TEM -2100F spectrometer. Nitrogen adsorption/desorption graphs were measured by a Micromeritics ASAP 2020M instrument. UV-Vis/DRS were carried out by the spectrometer (Cary 500 UV-Vis-NIR). Photoluminescence spectra were determined by a Varian Cary Eclipse

spectrometer. The samples were excited at a wavelength of 365 nm to measure the emission spectrum. Photocurrent measurements were measured on a CHI 630E electrochemical station.

<H2>2.3. Photocatalytic measurements

Photocatalytic degradation of RhB and PNP were conducted in a quartz photoreactor. The light source was provided by a PLS-SXE300 Xe lamp, and the light intensity was set at 150 mW cm^{-2} . Before Xe lamp irradiation, a suspension was obtained by mixing the solid catalyst (150 mg) and aqueous RhB solution (20 mg L^{-1} , 100 mL) or PNP solution (10 mg L^{-1} , 100 mL). The suspension was ultrasonicated for 10 mins and then stirred in the dark for 120 mins to achieve good dispersion and adsorption-desorption equilibrium between RhB molecules or PNP molecules and the catalyst. The concentrations of RhB or PNP in the reaction systems were measured using a Cary 500 UV-Vis-NIR spectrophotometer at $\lambda = 553 \text{ nm}$ and $\lambda = 317 \text{ nm}$, respectively.

<H1>3. Results and Discussion

<H2>3.1 Characterization of the materials

As presented in Fig. 1, X-ray diffraction (XRD) spectra of pure g-C₃N₄ and BiVO₄ materials showed the typical diffraction peaks ascribed to graphitic stacking structure of g-C₃N₄ and amonoclinic scheelite structure (PDF#14-0688) of BiVO₄, indicating the target materials are successfully synthesized [19]. While for the series of BiVO₄/g-C₃N₄ photocatalysts, both their characteristic structure patterns presented, which proved that BiVO₄ has been successfully introduced into g-C₃N₄ with their

structure well preserved, respectively. Meanwhile, with the increasing of BiVO₄ loading from 10%-30%, the diffraction peaks of g-C₃N₄ weakened, which may be due to the covering by the stronger diffraction patterns of BiVO₄ at higher loadings. Similar results have been reported by other research, that no typical crystalline peaks of g-C₃N₄ could be observed when the content of BiVO₄ on g-C₃N₄ is above 20% [20]. The surface areas of the BiVO₄ loaded g-C₃N₄ were semblable (24–32 m²/g) and similar with that of the pure g-C₃N₄ (42 m²/g), suggesting the structure and large specific surface areas of pure g-C₃N₄ were well sustained after BiVO₄ deposition. The FT-IR spectra of BiVO₄ doped g-C₃N₄ materials are shown in Fig. 2. For pure g-C₃N₄, sharp peak at 810 cm⁻¹ was found revealing the existence of heptazine units in the prepared g-C₃N₄. The bands located from 1640 to 1208 cm⁻¹ and the broad absorption peaks located from 3300 to 3000 cm⁻¹ are ascribed to the typical stretching modes of CN heterocycles and the stretching vibration of N-H bonds, respectively [21-23]. All these adsorption is the typical spectra for g-C₃N₄, in consistent with other literatures [21-23]. On the other hand, the pure BiVO₄ only showed one broad peak at 750cm⁻¹, which is also in line with the reported BiVO₄ FT-IR spectra, corresponding to the vibration of Bi-V bonds [24]. While for the series of BiVO₄/g-C₃N₄ photocatalysts, all characteristic absorption bands of pure BiVO₄ and g-C₃N₄ (stronger) appeared; with the increasing BiVO₄ loading, the characteristic absorption bands of pure BiVO₄ increased to some extent. This IR results combined with the XRD results, indicate that, after the adopting of BiVO₄ on g-C₃N₄ by sonification the structural integrity of g-C₃N₄ and BiVO₄ remains intact in the heterostructures.

The microstructures of asprepared BiVO₄ deposited g-C₃N₄ are revealed by TEM and SEM images (Fig. 3). SEM image of pure g-C₃N₄ displays a platelet-like morphology with a smooth surface (Fig. 3(a)). Obvious stacked pore structure was found between the platelet. Also, the TEM image (Fig. 3(b)) has shown that g-C₃N₄ is almost transparent, indicating its few-layer structure. On the other hand, the pure BiVO₄, which was well crystallized in the autoclave, was a polyhedral irregular particles with size of about hundred of nm to 1-2 μm as shown in Fig. 3(c) and (d). After introducing of BiVO₄, the sheet structure of g-C₃N₄ keeps well with irregular nanoparticles of BiVO₄ abundantly scattered (Fig. 3(e) and (f)). This result further confirmed the XRD finding that BiVO₄ have been successfully deposited on g-C₃N₄ and formed compressed heterojunctions composites instead of a simple physical mixture of each other. The well touched structure of the composites with an intimate interface will be benefit for the efficient charge transmission between BiVO₄ and g-C₃N₄ in visible light excitation, and thus improved their photocatalytic activity.

The XPS spectra of BiVO₄ doped g-C₃N₄ composites are presented in Fig. 4. The result indicates that main surface elements are C1s, N1s for pure g-C₃N₄, and Bi4f, V2p, and O1s for pure BiVO₄, respectively. After BiVO₄ introduced to g-C₃N₄, 10 wt.% BiVO₄/g-C₃N₄ exhibited all of the above elements but V2p. Basically, the C1s binding (Fig. 4B) of pure g-C₃N₄ and 10 wt.% BiVO₄/g-C₃N₄ is quite similar. However, N1s spectra (Fig. 4C) of g-C₃N₄ and 10 wt.% BiVO₄/g-C₃N₄ presents obvious difference. The first and the second contribution of N1s binding energy for pure g-C₃N₄ located at 398.1 eV and 399.1 eV, corresponding to sp²-hybridized

nitrogen (C=N-C) and tertiary nitride (N-C₃) group of g-C₃N₄ [25]. As for 10 wt.% BiVO₄/g-C₃N₄ composite, the N-C₃ binding energy shifts to higher level (about 1.2 eV). This may be caused by the interaction with BiVO₄ inducing C1s and N1s orbitals of g-C₃N₄ to the inner shift [20]. Furthermore, Bi 4f spectra over g-C₃N₄ and 10 wt.% BiVO₄/g-C₃N₄ (Fig. 4D) clearly presented the Bi 4f binding energies of pure BiVO₄, greatly shift to lower binding energy (about 0.6 eV) after BiVO₄ deposition on g-C₃N₄. These XPS analysis confirmed the above XRD and TEM results and clearly proved that compressed heterojunctions composites have been formed between g-C₃N₄ and BiVO₄ instead of a simple physical mixture.

Fig. 5 illustrates the UV-Vis spectra of the BiVO₄-g-C₃N₄ composites. As shown, the absorption edge of g-C₃N₄ is about 460 nm, and the bandgap is estimated to be 2.7 eV, in accordance with the literature results [26]. Pure BiVO₄ have much stronger absorption bands in visible-light and UV regions with steeper shape compared with g-C₃N₄, indicating a direct energy band gap [27]. As estimated, the absorption edge of pure BiVO₄ is around 525 nm, and its band gap is calculated to be 2.36 eV, also in accordance with the literature [28]. Meanwhile, the series of BiVO₄-doped g-C₃N₄ all shows strong absorption in visible-light and UV regions, with the adsorption range between absorption edge of pure BiVO₄ (525 nm) and g-C₃N₄ (460 nm). All of the band gaps of BiVO₄-doped g-C₃N₄ were slightly less than that of pure g-C₃N₄ (2.7 eV); the band gaps of the 10 wt.%, 20 wt.%, and 30 wt.% BiVO₄/g-C₃N₄ are estimated to be 2.67, 2.63, and 2.60 eV, respectively. These results indicate that after introducing of BiVO₄, the absorption edges of BiVO₄/g-C₃N₄ composites are shifted

to longer wavelength i.e. extend towards visible light range, which implies better optical absorption ability.

3.2 Photocatalytic performance

The photocatalytic activities of BiVO₄/g-C₃N₄ materials for RhB and PNP degradation are presented in Fig.6. As shown, all the samples reached the adsorption-desorption equilibrium for RhB molecules at about 30 min and the 10 wt.% BiVO₄/g-C₃N₄ sample has shown the highest adsorption rate of RhB (ca. 20%), almost twice of that of other photocatalysts (all at about 10%). After light on, pure BiVO₄ showed negligible low activity for RhB degradation, and pure g-C₃N₄ showed moderate high activity with RhB 50% degraded within 35 min. However, the BiVO₄ deposited g-C₃N₄ materials all exhibited much higher activity than C₃N₄, with 10 wt.% BiVO₄/g-C₃N₄ highest and 20 wt.% BiVO₄/g-C₃N₄ and 10 wt.% BiVO₄/g-C₃N₄ almost equally followed. This result indicate that the introducing of small amount of BiVO₄ could greatly increased the catalytic activities of C₃N₄ materials, and 10 wt.% BiVO₄/g-C₃N₄ exhibit the super photocatalytic activity with RhB 50% degraded within 10 min and complete degradation within 40 min. To further illustrate performance of the trace amount of BiVO₄ on the photocatalytic activity improvement of g-C₃N₄ materials and found out the optimized doping level of BiVO₄, the photocatalytic activity of g-C₃N₄ samples with lower BiVO₄ doping level than 10%, such as 5% and 7% are evaluated. As shown in Fig. S1, 10 wt.% BiVO₄/g-C₃N₄ still exhibited the highest activity among the three catalysts, followed by 7 wt.% BiVO₄/g-C₃N₄ and 5 wt.% BiVO₄/g-C₃N₄, respectively. This result indicates that 10% BiVO₄ is the optimized doping on the

photocatalytic activity improvement of g-C₃N₄ materials under the experiment condition, and it has showed high photocatalytic activity and great potential for further application, hence the followed discussion mainly concentrated on 10 wt.% BiVO₄/g-C₃N₄ material.

As shown in Fig. 6d, the characteristic adsorption of RhB (at 513 nm) over 10 wt.% BiVO₄/g-C₃N₄ under visible-light irradiation decreased constantly with extended irradiation time, with the RhB adsorption hardly observed after 40 min visible-light irradiation. Furthermore, this result is further confirmed by the RhB degradation rate calculated (Fig. 6c). The degradation rate of the catalysts followed the order: 10 wt.% BiVO₄/g-C₃N₄ (0.09307 min⁻¹) > 20 wt.% BiVO₄/g-C₃N₄ (0.07172 min⁻¹) > 30 wt.% BiVO₄/g-C₃N₄ (0.0658 min⁻¹) > g-C₃N₄ (0.02463 min⁻¹) > BiVO₄ (0.0425 min⁻¹). The 10 wt.% BiVO₄/g-C₃N₄ has about 4.8 times of degradation rate of pure g-C₃N₄ clearly proved the acitivity enhancement effect of BiVO₄ introducing.

For better evaluation of the visible-light catalytic property of these composites, Fig.6B showed photocatalytic performance of BiVO₄/g-C₃N₄ materials for the degradation of PNP, which is UV light insensitive. It is turned out the PNP degradation performance over these BiVO₄ deposited g-C₃N₄ catalysts is very similar with that of RhB degradation process. As shown in Fig. 6(b), with the introducing of BiVO₄, the photocatalysts exhibited much higher PNP conversion compared with pure g-C₃N₄. Also especially, 10 wt.% BiVO₄/g-C₃N₄ exhibited the highest photocatalytic activity, with PNP completely degraded within 120 min. Combined these degradation results of BiVO₄ and PNP, it could be concluded that the

introducing of BiVO₄ have greatly improved the catalytic activity of C₃N₄ materials and 10 wt.% BiVO₄/g-C₃N₄ photocatalyst exhibited the extraordinarily high photocatalytic activity for the organic pollutant degradation.

The high photocatalytic activity of 10 wt.% BiVO₄/g-C₃N₄ for the organic pollutant degradation motivated us to test its durability, which is also a crucial factor for the practical applications. Recycling reactions profiles (Fig. 7) showed that RhB can be completely degraded within 40 min in each cycle and no obvious activities decrease in catalytic activity was observed in the recycling reactions. Extraordinarily, the high photocatalytic activity and good stability of 10 wt.% BiVO₄/g-C₃N₄ for RhB degradation were comparable to or even superior to the most applied TiO₂ based photocatalysts [29-30]. As shown in the Fig. S2, under the same experiment conditions, the activity of 10 wt.% BiVO₄/g-C₃N₄ is much higher than pure TiO₂ photocatalysts. Thus, 10 wt.% BiVO₄/g-C₃N₄ seems great promising as a cost-effective photocatalyst for organic pollutant degradation in future application.

<H2>3.3 Role of BiVO₄ in photocatalytic activity enhancement on g-C₃N₄

The above characteristic results including XRD, FTIR and TEM/SEM clearly confirmed that BiVO₄ have been successfully deposited on the surface of g-C₃N₄ and formed well touched heterojunctions composites. The intimate interface between BiVO₄ and g-C₃N₄ in the composites greatly benefits for their UV-Vis absorption. As shown in UV-VIS DRS, the absorption edges of BiVO₄/g-C₃N₄ heterojunctions are prolonged towards visible light range, usually representative of better optical absorption ability [31]. The RhB decomposition results confirmed that the introducing

of BiVO₄ have greatly improved the catalytic activity of C₃N₄ catalysis. Thus, better optical absorption ability due to the well contacted structure in heterojunctions composites may play the first and most important role in the improvement of photocatalytic activity of g-C₃N₄. Furthermore, the heterojunctions composites, especially 10 wt.% BiVO₄/g-C₃N₄ has much larger BET-surface area (32.0 m²/g) than that of pure BiVO₄ (1.9 m²/g), indicating that the deposition of BiVO₄ on g-C₃N₄ greatly increased its adsorption of organic contaminants and thus improve its photocatalytic activity. However, the BET-surface area could not be the only factor deciding the adsorption performance of BiVO₄/g-C₃N₄ materials. As shown in Fig.6a, before light irradiation, the 10 wt.% BiVO₄/g-C₃N₄ sample, although has lower BET area than pure g-C₃N₄, already has shown much higher RhB adsorption rate (almost twice) compared with that of pure g-C₃N₄ and their RhB adsorption results all in consistent with their final photocatalytic performance under visible-light irradiation. Thus, we could deduce that there must be additional special adsorption effect over 10 wt.% BiVO₄/g-C₃N₄ besides simple physical adsorption. Hence, compared with pure g-C₃N₄, BiVO₄ deposited g-C₃N₄ exhibited better adsorption ability of organic contaminants, which would be another reason contributed for its high activity. Finally, the photoluminescence (PL) spectra of BiVO₄ deposited g-C₃N₄ is taken, as it is demonstrated that the separation efficiency of electron-hole pairs of the photocatalysts, revealed by fluorescence intensity in the PL spectra, is usually a very important factor influencing their activities [32]. Higher photocatalytic activity was usually associated with the photocatalysis exhibited lower fluorescence intensity,

which is representative of less recombination rate of photo-induced electron-hole pairs [20]. As shown in Fig. 8, PL emission intensities of the 10 wt.% BiVO₄/g-C₃N₄ is significantly lower than that of pure g-C₃N₄, suggesting the charge carriers recombination process of g-C₃N₄ can be suppressed in the presence of BiVO₄, and this may be another important factor for the improved photocatalytic activity after BiVO₄ introducing. This deduction is also directly proved by photoelectrochemistry test, which could intuitively display the complicated processes of generation, separation and migration of electrons and holes pairs [20]. During photoelectrochemistry test, the one with prompt photocurrent response corresponded to fast generation, separation and transportation of the photogenerated electrons in the light system [20]. As shown in Fig.9, all tested materials (as working electrodes) present sharp increased photocurrent responses immediately after light irradiation is on, and the photocurrents intensity are kept well during three cycles of light on-off intermittent irradiation. The 10 wt.% BiVO₄/g-C₃N₄/ITO electrodes present the highest photocurrent intensity, indicating the lowest electron-hole recombination rate. This result combined the photoluminescence spectra of BiVO₄ deposited g-C₃N₄ (Fig. 8) clearly demonstrated that low electron-hole recombination rate plays an important role in the photoactivity enhancement after BiVO₄ introducing.

<H2>3.4 Possible photocatalytic mechanism of BiVO₄/g-C₃N₄

The high photocatalytic activity and stability of 10wt.% BiVO₄/g-C₃N₄ for RhB degradation motivated us to investigate its photocatalytic mechanism in depth for

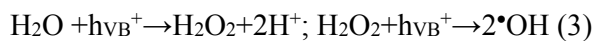
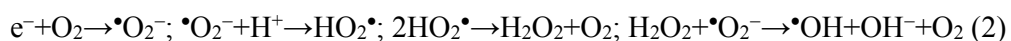
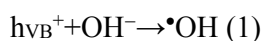
better application and understanding its activity enhancement further. Accordingly, free radical and hole captive test were carried out to identified the active species in the photocatalytic process of RhB degradation over pure g-C₃N₄ and 10wt.% BiVO₄/g-C₃N₄. As demonstrated by previous literatures [33,34], 1,4-benzoquinone (BQ), ethylene diamine tetraacetic acid (EDTA) and isopropyl alcohol (IPA) are used as •O₂⁻, h_{VB}⁺ and •OH scavengers, respectively.

For the process over pure g-C₃N₄ (Fig.10(a)), the presence of BQ (•O₂⁻ scavenger) and EDTA (h_{VB}⁺ scavenger) have great inhibition effect on the RhB degradation rate, while the presence of IPA (•OH scavenger) has no obvious change for RhB degradation. These results indicate that •O₂⁻ and h_{VB}⁺ play a major and minor role, respectively, in the photocatalytic RhB oxidization over g-C₃N₄, while h_{VB}⁺ hardly contributes. On the other hand, these scavengers displayed quite different influence on RhB degradation over the 10 wt.% BiVO₄/g-C₃N₄. As shown in Fig.10(b), besides •O₂⁻ and h_{VB}⁺, •OH is also active for BiVO₄/g-C₃N₄ photocatalytic process, which also corroborate the enhanced photocatalytic activity of BiVO₄/g-C₃N₄.

Based on the above analysis, a possible photocatalytic mechanism of the BiVO₄/g-C₃N₄ composites is proposed (Fig. 11). Both the redox potential of the valence band (E_{VB} = 2.36 eV) and the conduction band (E_{CB} = 0 eV) of BiVO₄ are more positive than those of g-C₃N₄ (E_{VB} = 1.4 eV and E_{CB} = -1.3 eV). The pure g-C₃N₄ and BiVO₄ can both be excited and produce photo-excited electrons and holes under visible light irradiation. Since the CB potential of g-C₃N₄ is lower than that of BiVO₄, the electrons in the CB of the g-C₃N₄ would transfer to the CB of BiVO₄. Similarly, the

VB potential of BiVO₄ is higher than that of g-C₃N₄, the holes in the VB of BiVO₄ would migrate to the VB of g-C₃N₄. As a consequence, the matching band potentials between BiVO₄ and g-C₃N₄ could effectively restrain the recombination of photogenerated electron-hole and improve the separation efficiency, which greatly promoted the photocatalytic degradation of RhB.

The electrons in the process of transferring from the CB of g-C₃N₄ to the CB of BiVO₄ could reduce O₂ to •O₂⁻, which together with the holes contributed on RhB degradation. Meanwhile, in the presence of water •OH radical is generated as the following possible reactions, and also plays an important role in RhB degradation:



<H1>4. Conclusions

BiVO₄/g-C₃N₄ heterostructure were facilely fabricated by a simple sonification method and were found to be highly active towards RhB and PNP degradation. Moreover, compared with the pure g-C₃N₄, these BiVO₄/g-C₃N₄ composites are much more active. The enhanced photocatalytic activity after BiVO₄ introducing to g-C₃N₄ is mainly attributed to the better optical absorption ability over the well contacted structure in heterojunctions, good adsorption ability of organic contaminants and lower recombination level of electron-hole pairs. In addition, over BiVO₄/g-C₃N₄, besides •O₂⁻ and hν_{VB}⁺ species (both active in BiVO₄/g-C₃N₄ and pure g-C₃N₄ system),

\bullet OH radical is also found to be active species for pollutants degradation; while in pure g-C₃N₄ system it hardly contributes. This result also corroborates the improved catalytic activity of 10 wt.% BiVO₄/g-C₃N₄. Furthermore, the most active 10 wt.% BiVO₄/g-C₃N₄ photocatalyst exhibits enough catalytic stability, showing great potential as cost-effective heterogeneous visible-light-driven photocatalyst for the purification of aqueous organic pollutants in future applications.

Acknowledgments

This work was financially supported by the Science and Technology Development Plan of Jilin Province (20140101162JC; 20120346; 20140520150JH) and National Natural Science Funds for Young Scholar (21307007).

<REF>References

<BIBL>

- [1] Y.X. Yang, Y.G. Guo, F.Y. Liu, X. Yuan, Y.H. Guo, S.Q. Zhang, W. Guo, M.X. Huo,¹; Preparation and enhanced visible-light photocatalytic activity of silver deposited graphitic carbon nitride plasmonic photocatalyst, *Appl. Catal. B: Environ.* 142-143 (2013) 828-837.
- [2] D.Q. Zhang, G.S. Li, J.C.¹; Yu, Inorganic Materials for Photocatalytic Water Disinfection, *J. Mater. Chem.* 20 (2010) 4529-4536.
- [3] T.T. Li, L.H. Zhao, Y.M. He, J. Cai, M.F. Luo, J.F. Lin,¹; Synthesis of g-C₃N₄/SmVO₄ composite photocatalyst with improved visible light photocatalytic activities in RhB degradation, *J. Appl. Catal. B: Environ.* 129 (2013) 255-263.
- [4] Y.L. Tian, B.B. Chang, Z.C. Yang, B.C. Zhou, F.N. Xi and X.P. Dong,¹; Graphitic carbon nitride-BiVO₄ heterojunctions: simple hydrothermal synthesis and high photocatalytic performances, *RSC. Adv.* 4 (2014) 4187.
- [5] S.C. Yan, Z.S. Li, Z.G. Zou,¹; Photodegradation performance of g-C₃N₄ fabricated by directly heating melamine, *Pubs. Acs. Org.* 25 (2009) 10397-10401.
- [6] S.M. Wang, D.L. Li, C. Sun, S.G. Yang, Y. Guan, H. He,¹; Synthesis and characterization of g-C₃N₄/Ag₃VO₄ composites with significantly enhanced visible-light photocatalytic activity for triphenylmethane dye degradation, *Appl.Catal. B: Environ.* 1144 (2014): 885-892.
- [7] P. Niu, L.L. Zhang, G. Liu, H.M. Cheng,¹; Graphene-like carbon nitride nanosheets for improved photocatalytic activities, *Adv. Funct. Mater.* 22(2012): 4763-4770.

- [8] C.C. Han, L. Ge, C. F. Chen, Y.J. Li, X.L. Xiao, Y.N. Zhang, L.L. Guo,¹; Novel visible light induced Co_3O_4 -g- C_3N_4 heterojunction photocatalysts for efficient degradation of methyl orange, *Appl. Catal. B: Environ.* 147(2014): 546-553.
- [9] X. H. Li, J.S. Chen, X.C. Wang, J.H. Sun,¹; Metal-free activation of dioxygen by graphene/g- C_3N_4 nanocomposites: functional dyads for selective oxidation of saturated hydrocarbons, *J. Am. Chem. Soc.* 133 (2011):8074-8077.
- [10] L.M. Sun, X. Zhao, C.J. Jia, Y.X. Zhou, X.F. Cheng, P. Li, W.L. Fan,¹; Enhanced visible-light photocatalytic activity of g- C_3N_4 - ZnWO_4 by fabricating a heterojunction: investigation based on experimental and theoretical studies, *J. Mater. Chem.* 22 (2012): 23428-23438.
- [11] L. Ge, C.C. Han, J. Liu,¹; Novel visible light-induced g- C_3N_4 / Bi_2WO_6 composite photocatalysts for efficient degradation of methyl orange, *Appl. Catal. B. Environ.* 108-109(2011):100-107.
- [12] F.J. Zhang, X.Z. Xie, S.F. Zhu, J. Liu, J. Zhang, S.F. Mei, W. Zhao,¹; A novel photofunctional g- C_3N_4 / Ag_3PO_4 bulk heterojunction for decolorization of RhB, *Chem. Eng. J.* 228 (2013): 435
- [13] A. Kudo,¹; Development of photocatalyst material for water splitting, *Int. J. Hydrogen Energy* 31 (2006) 197-202.
- [14] L. Chen, Q. Zhang, R. Huang, S. Yin, S. Luo and C. T. Au,¹; Porous peanut-like Bi_2O_3 - BiVO_4 composites with heterojunctions: one-step synthesis and their photocatalytic properties, *Dalton Trans.* 2012, 41, 9513-9518.
- [15] M.L. Guan, S.W. Hu, Y.J. Chen, S.M. Huang,¹; From hollowolive-shaped BiVO_4 to n-p core-shell BiVO_4 @ Bi_2O_3 microspheres controlled synthesis and enhanced visible-light-responsive photocatalytic properties, *Inorg. Chem.* 50(2011): 800-805.
- [16] Y.X. Ji, J.F. Cao, L.Q. Jiang, Y.H. Zhang, Z.G. Yi,¹; G- C_3N_4 / BiVO_4 composites with enhanced and stable visible light photocatalytic activity. *J. All. Com.* 590 (2014) 9-14.
- [17] F. Guo, W.L. Shi, X. Lin, G.B. Che, J.,¹; Hydrothermal synthesis of graphitic carbon nitride- BiVO_4 composites with enhanced visible light photocatalytic activities and the mechanism study, *Phys. Chem. Solids* 75(2014) 1217-1222.
- [18] Y. Vafeian, M. Haghghi, S. Aghamohammadi,¹; Ultrasound assisted dispersion of different amount of Ni over ZSM-5 used as nanostructured catalyst for hydrogen production via CO_2 reforming of methane, *Energ. Convers. Manage.* 76(2013) 1093-1103.
- [19] W. Liu, M.L. Wang, C.X. Xu, S.F. Chen, X.L. Fu,¹; Significantly enhanced visible-light photocatalytic activity of g- C_3N_4 via ZnO modification and the mechanism study, *J Mol Catal A-Chem.* 368-369 (2013) 9-15.
- [20] M. Ou, Q. Zhong, S.L. Zhang,¹; Synthesis and characterization of g- C_3N_4 / BiVO_4 composite photocatalysts with improved visible-light-driven photocatalytic performance. *J Sol-Gel Sci. Technol.* 72(2014):443-454.
- [21] S.C. Yan, Z.S. Li, Z.G. Zou,¹; Photodegradation Performance of g- C_3N_4 Fabricated by Directly Heating Melamine, *Langmuir* 25(17) (2009) 10397-10401.

- [22] J.H. Liu, T.K. Zhang, Z.C. Wang, G. Dawson, W. Chen,¹; Simple pyrolysis of urea into graphitic carbon nitride with recyclable adsorption and photocatalytic activity, *J. Mater. Chem.* 21 (2011) 14398-14401.
- [23] P. Niu, G. Liu, H.M. Cheng,¹; Nitrogen Vacancy-Promoted Photocatalytic Activity of Graphitic Carbon Nitride, *J. Phys. Chem. C* 116 (20) (2012) 11013-11018.
- [24] Z.M. Fang, Q. Hong, Z.H. Zhou, S.J. Dai, W.Z. Weng, H.L. Wan,¹; Oxidative dehydrogenation of propane over a series of low-temperature rare earth orthovanadate catalysts prepared by the nitrate method, *Catal. Lett.* 61 (1999) 39-44.
- [25] X.J. Wang, Q. Wang, F.T. Li, W.Y. Yang, Y. Zhao, Y.J. Hao, S.J. Liu,¹; Novel BiOCl-C₃N₄ heterojunction photocatalysts: in situ preparation via an ionic-liquid-assisted solvent-thermal route and their visible-light photocatalytic activities. *Chem. Eng. J.* 234 (2013): 361-371.
- [26] X.C. Wang, S. Blechert, M. Antonietti,¹; Polymeric Graphitic Carbon Nitride for Heterogeneous Photocatalysis, *ACS Catal.* 2 (2012) 1596-1606.
- [27] H.M. Luo, A.H. Mueller, T.M. McCleskey, A.K. Burrell, E. Bauer, Q.X. Jia,¹; Structural and photoelectrochemical properties of BiVO₄ thin films, *J. Phys. Chem. C.* 112 (2008): 6099-6102.
- [28] Y. Wang, X.C. Wang, M. A. Angew,¹; Polymeric Graphitic Carbon Nitride as a Heterogeneous Organocatalyst: From Photochemistry to Multipurpose Catalysis to Sustainable Chemistry, *Chem. Int. Ed.* 51 (2012) 68-69.
- [29] M.D. Hernandez-Alonso, F. Fresno, S. Suarez, J.M. Coronado,¹; Development of alternative photocatalysts to TiO₂: challenges and opportunities, *Energy Environ. Sci.* 2 (2009) 1231-1257.
- [30] H. Tong, S. Ouyang, Y. Bi, N. Umezawa, M. Oshikiri, J. Ye,¹; Nano-photocatalytic materials: Possibilities and challenges, *Adv. Mater.* 24 (2012) 229-251.
- [31] C. Zhang, Y.F. Zhu,¹; Synthesis of square Bi₂WO₆ nanoplates as high-activity visible -light-driven photocatalysts. *Chem. Mater.* 17(2005): 3537-3545.
- [32] X.L. Fu, W.M. Tang, L. Ji, S.F. Chen,¹; V₂O₅/Al₂O₃ composite photocatalyst: preparation, characterization, and the role of Al₂O₃, *Chem. Eng. J.* 180(2012)170-177.
- [33] C.S. Pan, Y.F. Zhu,¹; New type of BiPO₄ oxy-acid salt photocatalyst with high photocatalytic activity on degradation of dye, *Environ. Sci. Technol.* 44 (2010) 5570-5574.
- [34] C.C. Chen, Q. Wang, P.X. Lei, W.J. Song, W.H. Ma, J.C. Zhao,¹; Photodegradation of Dye Pollutants Catalyzed by Porous K₃PW₁₂O₄₀ under Visible Irradiation, *Environ. Sci. Technol.* 40(2006) 3965-3970.

</BIBL>

<Figure>Fig. 1 XRD patterns of g-C₃N₄, BiVO₄ and BiVO₄/g-C₃N₄ materials.

<Figure>Fig. 2 FT-IR spectra of g-C₃N₄, BiVO₄ and BiVO₄/g-C₃N₄ materials.

<Figure>Fig. 3 SEM images of g-C₃N₄ (a), BiVO₄ (c), 10 wt.% BiVO₄/g-C₃N₄ (e)

and TEM pictures of g-C₃N₄ (b), BiVO₄ (d), 10 wt.% BiVO₄/g-C₃N₄(f).

<Figure>Fig. 4 High-resolution XPS of (A) g-C₃N₄, BiVO₄ and 10 wt.% BiVO₄/g-C₃N₄; (B) C 1s, (C) N 1s and (D) Bi 4f binding energy regions.

<Figure>Fig. 5 UV-Vis/DRS (a) and the band gaps (b) of g-C₃N₄, BiVO₄ and BiVO₄/g-C₃N₄ materials.

<Figure>Fig. 6 Adsorption and photocatalytic property of BiVO₄ deposited g-C₃N₄ materials towards the degradation of RhB (a) and PNP (b); 400 nm < λ < 780 nm. (c) is the 10 wt.% BiVO₄/g-C₃N₄ corresponding reactive constant towards the degradation of RhB. (d) are the UV-Vis absorption spectra of RhB solution as a function of irradiation time during the photocatalytic process over the 10 wt.% BiVO₄/g-C₃N₄. Catalyst amount 100 mg; $c_0 = 20 \text{ mg L}^{-1}$, 10 mg L^{-1} ; volume 100 mL.

<Figure>Fig. 7 Recycling experiments over the 10 wt.% BiVO₄/g-C₃N₄ for RhB degradation of under visible-light irradiation. Catalyst amount 100 mg; $c_0 = 20 \text{ mg L}^{-1}$; volume 100 mL; 400 nm < λ < 780 nm.

<Figure>Fig. 8 Room temperature PL spectra of g-C₃N₄ and 10 wt.% BiVO₄/g-C₃N₄ under the excitation wavelength of 356 nm.

<Figure>Fig. 9 Photocurrent responses of g-C₃N₄ and 10 wt.% BiVO₄/g-C₃N₄ electrodes in 0.01 mol L⁻¹ Na₂SO₄ electrolyte solution under Xe irradiation.

<Figure>Fig. 10 The effect of scavengers on catalytic activity of g-C₃N₄ (a) and 10 wt.% BiVO₄/g-C₃N₄ (b) towards the degradation of RhB. Catalyst amount 100 mg; $c_0 = 20 \text{ mg L}^{-1}$; volume 100 mL; 400 nm < λ < 780 nm.

<Figure>Fig. 11 Proposed reaction scheme for photocatalytic process over BiVO₄ deposited g-C₃N₄ composites under visible-light irradiation.

TDENDOFOCTD